

1 **Manuscript**

2
3 **Enzymatic hydrolysis of polyester thin films at the nanoscale: effects of polyester**
4 **structure and enzyme active-site accessibility**

5
6 Michael Thomas Zumstein[†], Daniela Rechsteiner[†], Nicolas Roduner[†], Veronika Perz[‡],
7 Doris Ribitsch[‡]//, Georg M. Guebitz[‡]//, Hans-Peter E. Kohler[§], Kristopher McNeill[†],
8 and Michael Sander^{†,*}
9

10 [†] Institute of Biogeochemistry and Pollutant Dynamics, ETH Zurich, 8092 Zurich,
11 Switzerland
12

13 [§] Environmental Biochemistry Group; Environmental Microbiology, Swiss Federal
14 Institute of Aquatic Science and Technology (Eawag), 8600 Dübendorf, Switzerland
15

16 [‡] Austrian Centre of Industrial Biotechnology, ACIB, Konrad Lorenz Strasse 20, 3430
17 Tulln, Austria
18

19 ^{//} Institute of Environmental Biotechnology, University of Natural Resources and
20 Life Sciences, Vienna, Konrad Lorenz Strasse 20, 3430 Tulln, Austria
21

22
23
24 *To whom correspondence should be addressed:

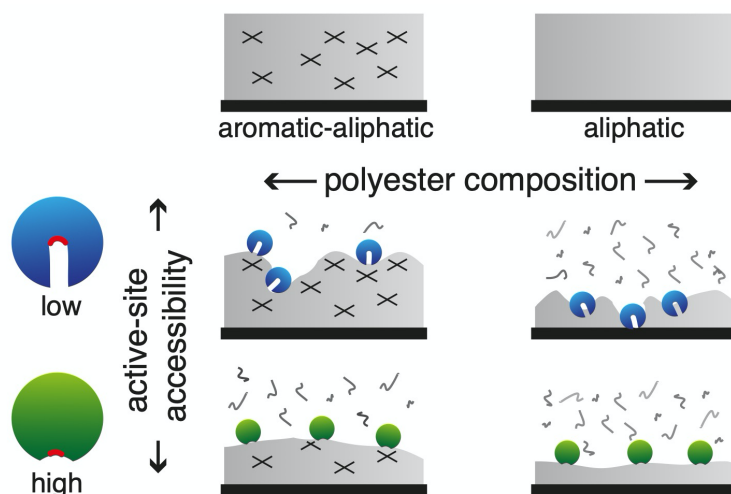
25 E-mail: michael.sander@env.ethz.ch,

26 Phone: +41-(0)44 6328314, Fax: +41 (0)44 633 1122
27

28

This document is the accepted manuscript version of the following article:

Zumstein, M. T., Rechsteiner, D., Roduner, N., Perz, V., Ribitsch, D., Guebitz, G. M., Kohler, H. P. E., McNeill, K., & Sander, M. (2017). Enzymatic hydrolysis of polyester thin films at the nanoscale: effects of polyester structure and enzyme active-site accessibility. *Environmental Science and Technology*, 51(13), 7476–7485.
<https://doi.org/10.1021/acs.est.7b01330>



29

30

Abstract

Biodegradable polyesters have a large potential to replace persistent polymers in numerous applications and to thereby reduce the accumulation of plastics in the environment. Ester hydrolysis by extracellular carboxylesterases is considered the rate-limiting step in polyester biodegradation. In this work, we systematically investigated the effects of polyester and carboxylesterase structure on the hydrolysis of nanometer-thin polyester films using a quartz-crystal microbalance with dissipation monitoring. Hydrolyzability increased with increasing polyester-chain flexibility as evidenced from differences in the hydrolysis rates and extents of aliphatic polyesters varying in the length of their dicarboxylic acid unit and of poly(butylene adipate co-terephthalate) (PBAT) polyesters varying in their terephthalate-to-adipate ratio by *Rhizopus oryzae* lipase and *Fusarium solani* cutinase. Nanoscale non-uniformities in the PBAT films affected enzymatic hydrolysis and were likely caused by domains with elevated terephthalate contents that impaired enzymatic hydrolysis. Yet, the cutinase completely hydrolyzed all PBAT films, including films with a terephthalate-to-adipate molar ratio of one, under environmentally relevant conditions (pH 6, 20 °C). A comparative analysis of the hydrolysis of two model polyesters by eight different carboxylesterases revealed increasing hydrolysis with increasing accessibility of the enzyme active site. Therefore, this work highlights the importance of both polyester and carboxylesterase structure to enzymatic polyester hydrolysis.

Introduction

The accumulation of persistent polymers in the environment is increasingly recognized as a major threat to both aquatic and terrestrial ecosystems.¹⁻⁶ In addition to

56 these environmental concerns, plastic accumulation may also have negative economic
57 impacts, including reduced crop yields from agricultural soils containing plastic
58 materials.⁷ These negative environmental and economic impacts call for strategies to
59 minimize plastic pollution and to advance towards a more sustainable use of polymer
60 materials. One promising strategy is to replace persistent polymers with biodegradable
61 materials, particularly for short-term uses, including packaging and agricultural
62 applications such as mulch films.⁸⁻¹¹

63 Aliphatic polyesters —synthesized from dicarboxylic acids and diols— and
64 aliphatic-aromatic co-polyesters —synthesized from aliphatic and aromatic
65 dicarboxylic acids and aliphatic diols— are two important classes of biodegradable
66 polymers.^{10,12} Aliphatic-aromatic co-polyesters are of particular commercial interest
67 because their physicochemical properties can be adapted to the requirement of a
68 specific application by changing the ratio of aliphatic to aromatic diacid
69 components.^{1,12-16} Depending on the application, biodegradable polyesters have
70 different end-of-life options, including landfilling, composting, de-polymerization for
71 recycling of monomers, and biodegradation in the soil in agricultural applications.^{9,17}
72 In all of these cases, the hydrolysis of ester bonds in the polyester is considered to be
73 the rate-limiting step in the overall biodegradation process.^{18,19} In pioneering work,
74 Tokiwa et al. demonstrated that extracellular microbial carboxylesterases catalyze the
75 hydrolysis of synthetic polyesters.²⁰ Since then, considerable research efforts have been
76 directed towards obtaining a fundamental understanding of enzymatic polyester
77 hydrolysis and towards identifying competent enzymes.²¹⁻²⁶

78 In previous studies, the enzymatic hydrolysis of polyesters was most commonly
79 measured either by quantifying the number of protons formed during carboxylic ester
80 hydrolysis with pH-stat titration²⁷ or by quantifying soluble polyester hydrolysis

products released into solution with dissolved organic carbon (DOC) measurements or high-performance liquid chromatography coupled to mass spectrometry (HPLC-MS) measurements.^{20,28-30} We recently introduced two complementary approaches: a high-throughput microplate method that is based on monitoring the co-hydrolysis of a fluorogenic ester probe embedded into the polyester,³¹ and an approach based on quartz-crystal microbalance with dissipation monitoring (QCM-D) measurements that allows real-time monitoring of the hydrolytic mass loss from polyester thin films.³² Compared to the other methods, the QCM-D approach is unique in that it provides insights into the dynamics of the enzymatic polyester hydrolysis at the nanometer scale.

Previous studies, in which pH-stat titration and the fluorogenic probe-based method were used, reported an inverse correlation between the rate of enzymatic polyester hydrolysis and the melting temperature, T_m , of the polyester.^{18,27,33,34} This finding was rationalized by considering T_m as a proxy for polyester chain flexibility: with decreasing T_m , the flexibility of polyester chains, and therefore also their propensity to enter the active site of a carboxylesterase, increased.^{18,27} Using the fluorogenic probe-based method, we recently extended on this chain-flexibility concept by showing that the rate of enzymatic hydrolysis of a set of aliphatic polyesters was additionally dependent on the accessibility of the active site of the carboxylesterase: while hydrolysis rates by *Rhizopus oryzae* lipase (RoL), for which the active site is located in a relatively deep pocket, showed a strong inverse correlation with T_m , hydrolysis rates by *Fusarium solani* cutinase (FsC), which has a more surface-exposed active site, showed a weaker inverse correlation with T_m .³¹ The importance of active-site structure is also evident from enzyme-engineering studies that demonstrated faster polyester hydrolysis by FsC after enlarging its active-site.^{35,36} Taken together, these findings point to a critical interplay between polyester-chain flexibility and enzyme

active-site accessibility in determining overall polyester hydrolysis. Therefore, studies that address this interplay by comparing the hydrolysis of a set of polyesters that systematically vary in structure by a diverse set of carboxylesterases are needed.

The objective of this work was to provide such a comprehensive analysis of the combined effect of polyester structure and enzyme active-site accessibility on enzymatic polyester hydrolysis. To this end, we performed QCM-D measurements to study the hydrolysis of nanometer-thick films of eight aliphatic polyesters and six aliphatic-aromatic co-polyesters by FsC and RoL, two hydrolases with very different active-site accessibilities. The aliphatic polyesters varied in the length of their diacid monomer, whereas the aliphatic-aromatic co-polyesters varied in their ratio of aromatic to aliphatic diacids. To assess the effect of active-site accessibility, we compared the hydrolysis of two selected polyesters by eight carboxylesterases of different classes.

Materials and Methods

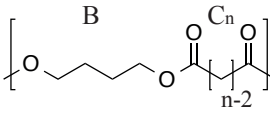
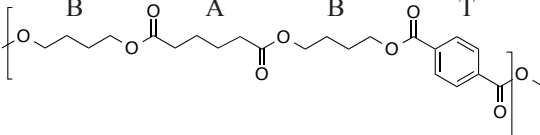
Chemicals and solutions. All chemicals used in this study are listed in the Supporting Information (SI). They were purchased from commercial suppliers and were used as received. All aqueous solutions were prepared in Milli-Q water (resistivity = 18.2 M Ω cm; Barnstead NANOpure Diamond) and contained 10 mM KCl as background electrolyte.

Polyesters. Table 1 shows the general chemical structures and physicochemical properties of the studied aliphatic polyesters (PBCn) and aliphatic-aromatic co-polyesters (PBATx). All polyesters were provided by BASF SE and were synthesized as previously described.^{37,38} While butanediol (B) was present in all aliphatic polyesters, they differed in the length of their dicarboxylic acid units (Cn, with n= number of carbon atoms). All aliphatic-aromatic co-polyesters contained B but were synthesized to have varying relative contents of terephthalate (T) to adipate (A),

131 expressed as the molar fraction of terephthalate to total diacid x (%) (i.e., $x =$
132 $T/(T+A) \cdot 100$).

133 **Table 1.** Generalized chemical structures and physicochemical properties of the tested
134 aliphatic polyesters (PBC n) and the aliphatic-aromatic co-polyesters (PBAT x). n and x
135 refer to the number of carbon atoms in the dicarboxylic acid components and the molar
136 fraction (%) of terephthalate (T) to total diacids (T + adipate (A)), respectively. T_m :
137 melting temperature, M_n : number average molecular weight, M_w : weight average
138 molecular weight, n.m.: not measurable. PBC6 and PBAT0 refer to the same polyester

material, also known as poly(butylene adipate) (PBA). The properties of the aliphatic polyesters were previously published.³¹

Aliphatic polyester (PBCn)				
				
Abbreviation	Number of carbon atoms in diacid (n)	T _m (°C)	M _n (g/mol)	M _w (g/mol)
PBC4	4	113.5	22700	112000
PBC6	6	58.7	19800	52100
PBC8	8	57.6	28100	94700
PBC9	9	53.2	25700	102000
PBC10	10	66.4	23700	95400
PBC12	12	75.5	28300	91300
PBC13	13	69.1	25700	78000
PBC18	18	84.9	n.m	n.m
Aliphatic-aromatic co-polyester (PBATx)				
				
Abbreviation	Fraction (%) of aromatic diacids (T/(A+T)) • 100	T _m (°C)	M _n (g/mol)	M _w (g/mol)
PBAT0	0	58.7	19800	52100
PBAT10	9.6	49.1	15600	51000
PBAT20	19.6	43.2	18400	56000
PBAT29	29.0	58.0	15900	48400
PBAT42	42.0	101.0	17600	52200
PBAT50	50.1	126.0	18300	56100

Enzymes. Table 2 lists the tested carboxylesterases, their source, and their hydrolytic activity under enzyme saturation (V_{max}) with the model ester substrate *para*-nitrophenyl butyrate (pNPB). We determined these activities using an approach adapted from Ribitsch et al.³⁹ In brief, we added carboxylesterase solution (20 μ L) and a pNPB-containing solution buffered at pH 6 (180 μ L; 50 mM 2-(*N*-morpholino)ethanesulfonic

acid (MES)) to the wells of a microplate (product number: 269620, Nunc). We independently verified that the obtained carboxylesterase and pNPB concentrations (5 mM pNPB) resulted in enzyme saturation. We subsequently followed the formation of the hydrolysis product, *para*-nitrophenol (pNP), by monitoring absorbance at 405 nm over time at 30 °C using a plate reader (Synergy HT, BioTek GmbH). The concentration of formed pNP was calculated based on the absorbance of pNP concentration standards that were measured on the same plate.

The hydrolysis of aliphatic polyesters (data in **Figure 1**) by FsC and RoL were conducted at enzyme activities of $1.8 \cdot 10^{-9}$ kat/mL and $7.7 \cdot 10^{-9}$ kat/mL, respectively (based on pNP formation). The hydrolysis of the aliphatic-aromatic co-polyesters (data in **Figure 2** and **3**) by FsC and RoL was investigated at an activity of $16.2 \cdot 10^{-9}$ kat/mL for both enzymes. We note that we employed two different RoL batches for the hydrolysis of the aliphatic polyesters (Sigma/62305) and aliphatic-aromatic co-polyesters (Sigma/80612). The use of two RoL batches and different enzyme concentrations impairs a direct comparison of the hydrolysis data in **Figure 1** and in **Figures 2** and **3**.

Table 2. Names, abbreviations, sources and catalytic activities of the used carboxylesterases. Activities were measured with the model ester substrate *para*-nitrophenyl butyrate (pNPB) at 30 °C and pH 6. An activity of 1 kat corresponds to the release of 1 mol of *para*-nitrophenol per second. We abbreviated the lipase of *Pelosinus*

167 *fermentans* as PefL (and not Pfl1 as originally published) to clearly delineate it from
 168 *Pseudomonas fluorescens* lipase, abbreviated as Pfl.

Abbreviation	Organism	Class	Supplier / product number	Activity on pNPB kat/mg, 10 ⁻⁹
FsC	<i>Fusarium solani</i>	cutinase	ChiralVision B.V. (Novozym 51032)	394 ± 14
RoL	<i>Rhizopus oryzae</i>	lipase	Sigma / 62305 Sigma / 80612	77 ± 4 66.9 ± 1.9
TcC	<i>Thermobifida cellulosilytica</i>	cutinase	expressed in <i>E.coli</i> ^a	4460 ± 200
CbE	<i>Clostridium botulinum</i>	esterase	expressed in <i>E.coli</i> ^a	649 ± 14
PefL	<i>Pelosinus fermentans</i>	lipase	expressed in <i>E.coli</i> ^a	611 ± 12
Pfl	<i>Pseudomonas fluorescens</i>	lipase	Sigma / 534730	35.3 ± 1.2
PcL	<i>Pseudomonas cepacia</i>	lipase	Sigma / 62309	61 ± 7
AnL	<i>Aspergillus niger</i>	lipase	Sigma / 62301	8.04 ± 0.21

169

170 ^aEnzymes were cloned and expressed in *Escherichia coli* as described in the literature:
 171 CbE (Cbotu_EstA, GenBank number: KP859619),²² PefL (Pfl1, KM377649),²⁴ and
 172 TcC (Thc_cut1, HQ147785).²⁹

173 **Polyester hydrolysis.** We used a QCM-D E4 system (Q-Sense, Sweden) with four
 174 flow cells to follow the enzymatic hydrolysis of polyester thin films coated onto QCM-
 175 D sensors.³² QCM-D is a piezo-acoustic resonator technique that monitors the changes
 176 in the resonance frequencies, Δf_i (Hz), and the energy dissipations, ΔD_i , of a piezo
 177 quartz crystal embedded into the QCM-D sensor. During the hydrolysis experiment,
 178 the fundamental tone ($i= 1$) as well as six oscillation overtones ($i=$ odd numbers
 179 between 3 and 13) were continuously measured. We converted measured Δf_i values into
 180 changes in the adlayer mass on the sensor surface, Δm (ng/cm²), using the Sauerbrey
 181 equation (Eq. 1):

$$182 \quad \Delta m = C \cdot -\frac{\Delta f_i}{i} \quad \text{Eq. 1}$$

183 where C ($=17.7 \text{ ng} \cdot \text{cm}^{-2} \cdot \text{Hz}^{-1}$) is the sensor-specific mass sensitivity constant.

184 The fifth overtone ($i= 5$) was used for plots and calculations.

185 For the preparation of polyester thin films, the polyesters were first dissolved in
 186 chloroform to a final concentration of 0.5% (w/w). We then transferred 40 μL of the

polyester solution onto a QCM-D sensor (QSX 301, Microvacuum) mounted on a spin coater (WS-650MZ-23NPP, Laurell Technologies), followed by spinning the sensor for 1 min at 4000 rpm with an acceleration of $1500 \text{ rpm} \cdot \text{s}^{-1}$. The mass of each coated film was calculated from the decrease in the resonance frequencies of the sensor before and after the coating step, both measured on the QCM-D in air at 20 °C. All spin-coated films had thicknesses of around 80 nm, consistent with previous work.³²

Each polyester-coated QCM-D sensor was pre-equilibrated to the solution used in hydrolysis experiments (i.e., 3 mM sodium phosphate, pH 6, filtered through 0.2 μm cellulose acetate syringe filters) by immersing the sensor in a solution of the same composition for 14 h at 25 °C. We subsequently mounted the sensor into the flow cell of the QCM-D instrument and ran the experimental solution over the sensor at a constant volumetric flow rate (20 $\mu\text{L}/\text{min}$) and a constant temperature. Upon attaining constant Δf_i and ΔD_i values, we switched to solutions that contained one of the carboxylesterases while all other solution parameters remained the same. Hydrolysis of the polyesters led to increasing resonance frequencies (i.e. decreasing adlayer masses) and was followed until constant Δf_i and ΔD_i values were re-attained. We subsequently removed the sensors from the flow cells, washed them by dipping them into Milli-Q water, and finally dried them in a N_2 stream. To determine the fraction of the coated polyester mass that was removed by enzymatic hydrolysis, we determined the resonance frequency of each dried sensor in air at 20 °C after hydrolysis and compared this frequency to those measured prior to hydrolysis. We cleaned the flow cells and sensors after each experiment following a previously published method,⁴⁰ as explained in the SI.

Results and Discussion

Polyester hydrolysis. Aliphatic polyesters. **Figures 1a** and **1b** show the results of representative QCM-D experiments for the hydrolysis of PBC4, PBC6, PBC10 and PBC18 by FsC (panel a) and RoL (panel b). The results of representative hydrolysis experiments of the remaining polyesters (i.e., PBC8, PBC9, PBC12 and PBC13) are provided in **Figure S1**. The hydrolysis dynamics of PBC8 and PBC9 and of PBC12 and PBC13 were similar to those of PBC6 and PBC10, respectively. Hydrolysis experiments were highly reproducible, as shown exemplarily by results from duplicate hydrolysis experiments of PBC8 by FsC and RoL (**Figure S2**). Furthermore, the QCM-D approach was highly sensitive: the hydrolysis of PBC4 by RoL was readily detectable by QCM-D (**Figure 1b**), whereas PBC4 hydrolysis by lipases was too slow to be detectable in earlier studies in which other techniques were used.^{27,31}

The adlayer mass of all PBCn films was constant in enzyme-free solutions at $t < 0$ h (**Figures 1a,b** and **S1**). Furthermore, we illustrated for PBC6 that the mass of a spin-coated polyester film did not change during its exposure to an enzyme-free buffer solution for 24 h (**Figure S3**). These findings demonstrated that non-enzymatic hydrolysis of PBCn was negligible. Adding FsC and RoL at $t = 0$ h led to changes in the adlayer mass that differed between the two enzymes. A decreasing adlayer mass indicated hydrolysis of the polyesters and the release of water-soluble hydrolysis products into solution.³² We used ^1H nuclear magnetic resonance (NMR) to confirm the presence of hydrolysis products in the solutions eluting from the QCM-D flow through cells during the hydrolysis of PBC6 films by both RoL and FsC (**Figure S4**).

The addition of FsC led to immediate decreases in the adlayer mass of all PBCn films except for PBC18 (**Figures 1a** and **S1a**). The initial mass-loss rates were highest for PBC6, PBC8, and PBC9 films. These rates remained high until the adlayer mass leveled off, approximately 1.5 h after FsC addition, at constant final values that

corresponded to (close to) complete film removal as discussed below. The mass progress curves of PBC4, PBC10, PBC12, and PBC13 showed two consecutive phases. The first phase had a smaller mass-loss rate and continued until approximately $1 \mu\text{g}\cdot\text{cm}^{-2}$ of the adlayer mass was removed. The second phase had a higher mass-loss rate and continued until the adlayer mass leveled off at final stable values. The decrease in adlayer mass was slowest for PBC18 films and showed three consecutive phases. An initial phase with a low mass-loss rate was followed by a second phase during which the adlayer mass increased. Given that QCM-D senses the mass of adlayer-associated water,^{32,41,42} we attribute this increase to the incorporation of water (and enzyme molecules) into the film during this stage of the hydrolysis.³² This explanation is supported by a pronounced increase in the energy dissipation values of the adlayer and hence a decrease in adlayer rigidity during this phase (**Figure S5**). The third and final phase was characterized by a continuous loss of adlayer mass and a decrease in the dissipation until they both leveled off at stable final values (inset **Figure 1a**).

In comparison to FsC, the addition of RoL caused small initial increases in the adlayer mass for all PBCn films after which the adlayer mass remained constant for some time. These mass increases likely resulted from the adsorption of RoL molecules to the PBCn film surfaces. For all polyesters, the first phase of constant adlayer mass transitioned into a phase with a high mass-loss rate. As argued in more detail below, polyester hydrolysis by RoL likely occurred primarily in the vertical direction into the thin films. Therefore, the release of hydrolysis products during the first phase was probably compensated by the incorporation of water into the film, resulting in only small changes in the adlayer mass. The sharp transition into the second phase occurred when the pre-hydrolyzed film became sufficiently unstable and was therefore rapidly

removed from the sensor. For all polyesters, the mass progress curves ultimately leveled off at stable values that corresponded to extensive film hydrolysis, as explained below.

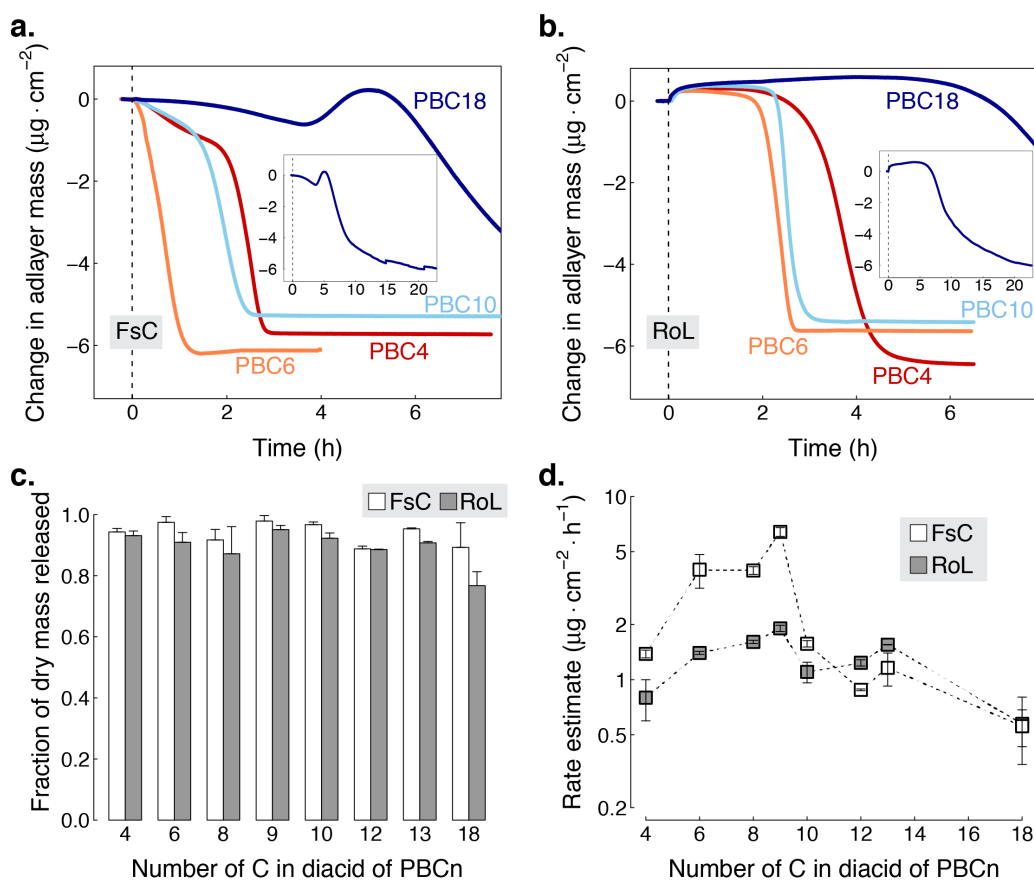


Figure 1. Enzymatic hydrolysis of a set of aliphatic polyesters that all contained butanediol (B) but dicarboxylic acid components with varying lengths (C_n) (PBC $_n$ with n = number of carbon atoms in diacid; see Table 1 for details) by *Fusarium solani* cutinase (FsC) and *Rhizopus oryzae* lipase (RoL) at pH 6 and 30 °C, as determined by quartz-crystal microbalance with dissipation monitoring (QCM-D) measurements. **a.** and **b.** Changes in the adlayer mass of PBC4, PBC6, PBC10, and PBC18 films (complete curves for PBC18 shown in the insets) during their enzymatic hydrolysis by FsC (a.) and RoL (b.). Enzymes were continuously run over the sensors starting at time $t = 0$ h, as indicated by the vertical dashed lines. **c.** Fraction (%) of the initially coated polyester film mass that was removed during the hydrolysis experiment. **d.** Estimated rates of enzymatic polyester hydrolysis. Error bars in c. and d. represent deviations of duplicates from their mean.

To determine the extents of polyester hydrolysis when adlayer masses leveled off at final stable values, we determined the dry mass of each sensor after the hydrolysis experiment and compared it to its mass before and after spin coating. For all PBC $_n$ and both enzymes, the fraction of the initially coated polyester mass that was removed was close to 100% (**Figure 1c**), suggesting extensive (if not complete) transformation of all

films into soluble hydrolysis products. Fractional mass losses slightly smaller than 100% likely resulted from positive mass contributions of enzymes that adsorbed to the gold surface of the QCM-D sensor after hydrolytic removal of the polyester films.³² Fractional mass losses close to 100% imply that the differences in the end points of the mass progress curves between PBCn films (**Figures 1a,b** and **S1a,b**) reflected differences in the spin-coated masses and not in the extents of hydrolysis.

To compare the hydrolysis rates for all polyester-enzyme combinations, we approximated the rates with the time that was required to remove half of the initially coated adlayer mass (i.e., estimated rate with units of $\mu\text{g}\cdot\text{cm}^{-2}\cdot\text{h}^{-1}$). The estimated rates for FsC-mediated hydrolysis of aliphatic polyesters decreased in the order $\text{PBC9} > \text{PBC6} \approx \text{PBC8} > \text{PBC10} \approx \text{PBC4} \approx \text{PBC13} \approx \text{PBC12} > \text{PBC18}$ (**Figure 1d**). For RoL, the estimated rates were slightly higher for polyesters with intermediate-length diacids (i.e., PBC6, PBC8, PBC9, PBC10, PBC12, and PBC13) than for the two polyesters with the shortest and longest diacid component (i.e., PBC4 and PBC18).

Aliphatic-aromatic co-polyesters. **Figures 2a** and **2b** show representative mass progress curves during the hydrolysis of PBATx films by FsC and RoL, respectively. Constant adlayer masses prior to enzyme addition at $t = 0$ min again implied that non-enzymatic hydrolysis was negligible. Good agreement between duplicate hydrolysis experiments of PBAT29 films with both FsC and RoL (**Figure S6**) demonstrated that QCM-D measurements were highly reproducible also for PBAT films.

Adding FsC to PBATx films resulted in an immediate adlayer mass loss (**Figure 2a**) indicating a fast onset of film hydrolysis by FsC. All mass progress curves eventually leveled off at similar final values. At these final values, almost all of the initially coated polyester mass was removed (i.e., fractional mass losses close to 100%) (**Figure 2c**), suggesting extensive (if not complete) hydrolysis of PBATx films by FsC.

The estimated hydrolysis rates, determined as described above, were similar for PBAT0, PBAT10, and PBAT20 but successively decreased with increasing terephthalate contents from PBAT29 to PBAT42 and to PBAT50 (Figure 2d).

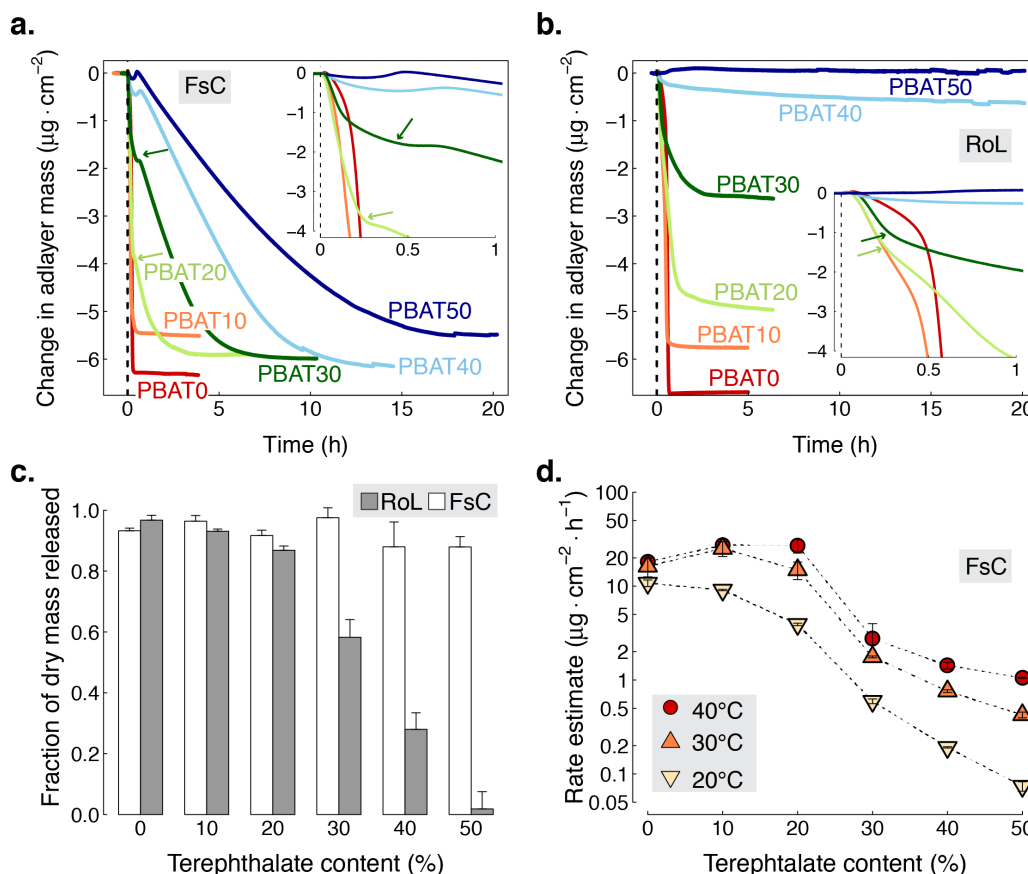


Figure 2. Hydrolysis of poly(butylene adipate co-terephthalate) (PBATx) thin films by *Fusarium solani* cutinase (FsC) and *Rhizopus oryzae* lipase (RoL) at pH 6, as measured with a quartz-crystal microbalance with dissipation monitoring (QCM-D). The different PBATx polyesters varied in the molar fraction of the aromatic diacid terephthalate (T) to the aliphatic diacid adipate (A) (i.e., $x = T/(A+T) \cdot 100$). **a.** and **b.** Changes in the adlayer mass during the hydrolysis of PBATx thin films by FsC (**a.**) and RoL (**b.**) at 30 °C. Enzymes were added at time $t = 0$ h, as indicated by the vertical dashed lines. The insets show the adlayer mass progress curves within the first hour of carboxylesterase addition. **c.** Fraction (%) of initially coated dry polyester mass that was removed during the hydrolysis experiments. **d.** Estimated rates for the hydrolysis of PBATx films by FsC at three different experimental temperatures. Error bars in panels c. and d. represent deviations of duplicate measurements from their mean.

Compared to the hydrolysis by FsC, the hydrolysis of PBATx films by RoL showed a much stronger dependence on the terephthalate content (Figure 2b). Adlayer masses of PBAT0 and PBAT10 films decreased immediately after adding RoL and leveled off at constant final masses within less than one hour after RoL addition. These

final values corresponded to almost complete polyester film removal (**Figure 2c**). We note that the differences in the mass progress curves during hydrolysis of PBAT0 (=PBC6) by RoL in **Figures 1** and **2** are due to different RoL concentrations used for these experiments (see Materials and Methods section). PBAT20 and PBAT29 films showed high initial mass-loss rates that decreased when approximately 1.5 and 1 $\mu\text{g}\cdot\text{cm}^{-2}$ of adlayer mass had been removed, respectively (arrows in **Figure 2b**). The mass progress curves leveled off at final values, which corresponded to incomplete hydrolysis of the PBAT20 and PBAT29 films (**Figure 2c**). Continuous exposure of PBAT42 and PBAT50 films to RoL over 20 h resulted in only small and no mass losses, respectively (**Figure 2b**). Consistently, the fractional mass loss measured on dried sensors at the end of the experiments was only 28 and 2% of the spin-coated PBAT42 and PBAT50 films, respectively (**Figure 2c**). Due to the incomplete hydrolysis of films of PBAT20, PBAT29, PBAT42 and PBAT50 by RoL, we did not estimate hydrolysis rates for these experiments.

Mechanistic interpretation of polyester hydrolysis data. The experimental data clearly show that rates and extents of polyester hydrolysis were dependent on both the chemical structure of the polyesters and the type of carboxylesterase used. These two important factors on enzymatic polyester hydrolysis are separately discussed below.

Effect of polyester structure. Previous work has shown increasing enzymatic hydrolysis rates of aliphatic polyesters and aliphatic-aromatic co-polyesters with decreasing polyester T_m .^{27,31,34} This trend was ascribed to increasing polyester chain flexibility with decreasing T_m and, as a consequence, increasing propensity for ester bonds to reach into the active site of hydrolases adsorbed to the polyester surface. While it was technically unfeasible to measure T_m for the spin-coated thin films, we plotted the estimated hydrolysis rates of PBCn and PBATx films by RoL and FsC to the T_m

values determined on granules of the respective polyesters (**Table 1**). Hydrolysis of the PBCn films by RoL showed only a slight overall rate increase with decreasing polyester T_m (**Figure S7**). For these polyesters, the T_m values measured on polyester granules therefore were relatively poor predictors for thin film hydrolysis rates. The hydrolysis of PBCn and PBATx films by FsC (**Figures S7 and S8**) showed clearer trends of increasing rates with decreasing polyester T_m . At the same time, there were notable deviations from these trends. The hydrolysis rates of PBC4—the aliphatic polyester with the highest T_m —by FsC was high relative to the polyesters with lower T_m (**Figures S7**). Also, the hydrolysis rate of PBAT0 by FsC was significantly higher than of PBAT29, while both polyesters had similar T_m values (**Figure S8**). Despite the apparent limitations in relating thin film hydrolysis rates to bulk polyester properties, the overall trends between rates and T_m of all studied systems were consistent with the chain-flexibility hypothesis.

As compared to experiments with macroscopic polyester materials, working with polyester thin films on a QCM-D platform has the unique advantage that enzymatic hydrolysis can be studied directly at the nanoscale. This advantage allows for a molecular-level mechanistic interpretation of the effect of PBATx structure on hydrolysis. The initial phases of PBATx hydrolysis by FsC showed distinct features in the mass progress curves that depended on the terephthalate contents of the films (**Figure 2a**). For films with low terephthalate contents (i.e., PBAT0 and PBAT10), the adlayer masses continuously decreased with a high mass loss rate until a final stable mass was attained, suggesting that the activity of FsC on these polyesters remained high and approximately constant until the entire film was hydrolytically removed from the sensor. By contrast, PBAT20 and PBAT29 films only showed a high mass-loss rate until approximately 3.8 and $1.8 \mu\text{g}\cdot\text{cm}^{-2}$ of the coated masses had been removed,

respectively (see arrows in inset of **Figure 2a**). Then, the mass-loss rates decreased and hydrolysis transitioned into a second phase with smaller mass-loss rates. The adlayer mass of PBAT42 and PBAT50 decreased only slightly after FsC addition, and rapidly transitioned into the phase with comparatively low mass-loss rates.

These transitions from phases of fast hydrolysis into phases of slower hydrolysis imply a non-uniformity in the PBATx films at the nanometer scale. As the terephthalate contents increased, the mass fractions of the PBATx films that were readily hydrolyzable decreased. We ascribe the initial phase with a comparatively high mass-loss rate to the hydrolysis of PBAT domains with relatively low terephthalate-to-adipate ratios. This fast hydrolysis progressed until the film surface became enriched in domains with higher terephthalate-to-adipate ratios, which slowed down subsequent hydrolysis. This explanation is also consistent with the pronounced decrease in the extent of PBATx hydrolysis by RoL with increasing terephthalate content. Apparently, only domains with low terephthalate-to-adipate ratios were hydrolyzable by RoL, whereas the polyester chains in domains with high terephthalate contents were not flexible enough to reach into the active site of RoL (**Figure 2b**). The adlayer mass that was released at the end of the phase of fast hydrolysis correlated well between FsC and RoL. This correlation indicated that the non-uniformity in the films affected hydrolysis by both enzymes (**Figure S9**).

To support that PBATx films contained terephthalate-rich domains with reduced chain flexibilities, we complemented the hydrolysis experiments of PBATx films at $T_{\text{exp}} = 30^{\circ}\text{C}$ with additional experiments at 20°C and 40°C (**Figures S10 and S11**). We found that increasing T_{exp} increased the fraction of the PBAT films that were readily hydrolyzable by both enzymes (**Figures S9 and S10**), consistent with a temperature-induced increase in the flexibility of the polyester chains in the terephthalate-enriched

domains of these polymers. Increasing T_{exp} also increased the estimated rates of PBATx hydrolysis by FsC (**Figures 2d** and **S6**). It is likely that part of this rate increase resulted from an increase in the activity of FsC with T_{exp} . However, the rate increase with increasing T_{exp} was more pronounced for the high- T_m polyesters (PBAT42 and PBAT50) than for low- T_m polyesters (PBAT0, PBAT10) (**Figure S12**). This finding further supports that PBATx films contained domains with high terephthalate contents and impaired enzymatic hydrolyzability.

To further support our explanation for film non-uniformity, we calculated the probability of oligomeric sequences with a defined number of terephthalate monomers in the PBATx films, assuming a random incorporation of adipate and terephthalate into the polyester chain during synthesis (see SI for details). The calculated probabilities of having two or fewer terephthalate units in a sequence of eight butanediol-diacid dimers are 81, 58, 28, and 14 % for PBAT20, PBAT29, PBAT42, and PBAT50, respectively (**Figure S13**). These probabilities are in good agreement with the mass fractions of the PBAT polyesters that were readily hydrolyzed, suggesting that decreased hydrolyzability was likely caused by 16-mers with three or more terephthalate units.

Taken together, the QCM-D data and theoretical calculations strongly support that the presence of terephthalate-enriched domains in the PBATx polymers impaired hydrolysis. On a molecular level, impaired hydrolysis presumably resulted from a restricted flexibility of the polyester chains in domains with higher terephthalate contents.³⁴ Slower enzymatic hydrolysis of ester bonds between butanediol and terephthalate than between butanediol and adipate, as previously reported for lipases,^{23,43} may have further contributed to the overall impaired hydrolysis of terephthalate-enriched domains.

Effect of type of esterase. While all tested aliphatic polyesters PBCn were completely hydrolyzed by both FsC and RoL, the mass progress curves were very different for the two enzymes. FsC addition resulted in an immediate onset of adlayer mass loss, whereas RoL addition was followed by an extended phase without mass loss (**Figure 1**). We propose that this phase during RoL-mediated hydrolysis resulted from an initial hydrolysis of a few ester bonds on the polyester surface forming negatively charged carboxylate groups which subsequently diminished the activity of RoL on ester bonds on the polyester surface in close proximity to the formed carboxylate moieties.³² This explanation builds on previous work that showed that lipases—in contrast to cutinases—commonly need to interact with an apolar surface to become fully active.^{15,44,45} In this process, called interfacial activation, a conformational change in the lipase leads to the repositioning of a lid-like peptide structure and results in the exposition of the pocket with the active site.⁴⁶ Consistent with this explanation, we showed in pH-stat titration experiments that solvent-cast PBC6 films were hydrolyzed by RoL to dissolved dimers and not monomers (**Figure S14**), implying impaired RoL activity on ester bonds close to negatively charged carboxylate groups. By comparison, FsC hydrolyzed all ester bonds of the PBC6 film to form monomers (**Figure S14**). Impaired RoL activity on charged polyester surfaces is also consistent with slower hydrolysis of aliphatic polyesters with short diacids (i.e., PBC4 to PBC10) by RoL than by FsC, while hydrolysis rates for the three aliphatic polyesters with the long diacids (i.e., PBC12, PBC13, and PBC18) were similar for the two enzymes.

The lipase-specific interfacial activation mechanism may also have favored vertical hydrolysis into the polyester film over lateral surface hydrolysis. Preferential vertical hydrolysis would help rationalize the mass progress curves during the hydrolysis of PBCn films by RoL. First, hydrolysis by RoL, as compared to hydrolysis

by FsC, would require more time to form hydrolysis products of a sufficiently small size to detach from the PBCn film surfaces. Secondly, if vertical hydrolysis by RoL prevailed, mass loss due to the release of hydrolysis products would be compensated by the incorporation of water into the film. This water incorporation may have contributed to the initial phase with constant adlayer masses. Third, preferential hydrolysis in the vertical direction would ultimately result in structurally unstable films susceptible to fast detachment from the sensor surface. The formation of such films would explain the sharp transition from the initial phase without substantial mass loss into the second phase with high mass-loss rates (**Figures 1b** and **S1b**).

All aliphatic-aromatic co-polyesters were completely hydrolyzed by FsC, whereas the hydrolysis of PBAT variants with higher terephthalate contents (i.e., PBAT29, PBAT42 and PBAT50) by RoL was incomplete. The crystallographic structures of the two enzymes show that the active site of RoL is located in a relatively deep pocket, whereas the active site of FsC is more surface-exposed.³¹ We recently argued that this difference in the architecture of the active-site resulted in a more pronounced dependence on polyester-chain flexibility on the formation of the enzyme-substrate complex for RoL than for FsC. This argument is fully consistent with the finding of impaired hydrolysis of terephthalate-rich domains in PBATx by RoL in this work.

To place the results obtained by FsC and RoL into a larger context and to further assess the importance of active site accessibility, we tested the hydrolyzability of PBAT0 (= PBC6) and PBAT50, the two end members of the PBATx set, by six additional microbial carboxylesterases (**Figures 3** and **S15; Table 2**). In this set, the cutinase FsC and the two lipases RoL and AnL were of fungal origin. The second cutinase TcC, the three lipases PcL, PfL, and PefL, and the tested esterase CbE were of

bacterial origin. All eight enzymes were used in concentrations that resulted in the same activities on the model substrate para-nitrophenyl butyrate.

Five enzymes (CbE, PcL, TcC in addition to RoL and FsC) rapidly and extensively hydrolyzed PBAT0 (**Figure 3a**). Larger dissipation values were observed for PBAT0 films during hydrolysis by the lipases than by the cutinases and the esterase (**Figure S16**), supporting the formation of structurally instable, water-rich film intermediates during lipase-mediated hydrolysis. Exposure of PBAT0 films to the remaining three hydrolases PefL, Pfl, or AnL resulted in initial increases in adlayer mass, presumably due to enzyme adsorption to the PBC6 surfaces, followed by a comparatively slow mass loss. Relative to their activity on para-nitrophenyl butyrate, these three enzymes therefore had considerably lower activities on PBAT0 than the other enzymes.

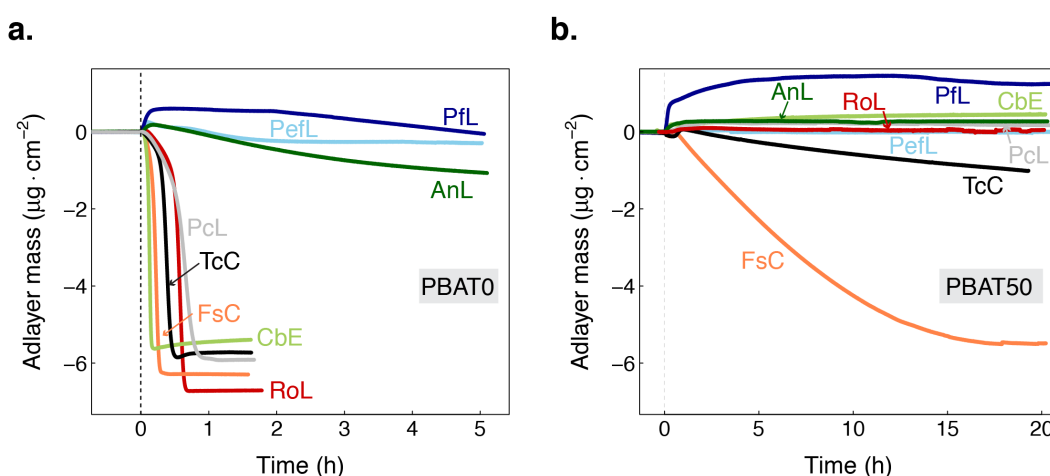


Figure 3. Hydrolysis of films of poly(butylene adipate) (PBAT0= PBC6) (panel **a.**) and poly(butylene adipate co-terephthalate) with a terephthalate content of 50 % relative to the total diacid content (i.e., PBAT50 (panel **b.**) by a set of carboxylesterases (abbreviations of enzymes shown next to curves, see Table 1 for full names and details) at pH 6 and 30 °C as investigated by quartz-crystal microbalance with dissipation monitoring (QCM-D) measurements. For clarity, we show one representative measurement of duplicates for each enzyme-polyester combination.

Among the eight tested hydrolases, only FsC extensively hydrolyzed PBAT50 films within 20 h (**Figure 3b**). A slower but significant decrease in the PBAT50 adlayer mass was detected during hydrolysis by TcC, the second tested cutinase. Neither the

500 esterase nor the five lipases hydrolyzed the PBAT50 films to detectable amounts over
501 the course of the 20 h experiment. These pronounced differences in the activities of the
502 tested carboxylesterases on both films were confirmed by fractional losses of adlayer
503 mass determined on dried sensors after the hydrolysis experiments (**Figure S15**).
504 Similar to RoL, an increase in the terephthalate contents from PBAT0 to PBAT50
505 largely impaired the hydrolysis by CbE and by PcL. The findings of PBAT50
506 hydrolysis by TcC and of faster PBAT0 than PBAT50 hydrolysis by CbE are in good
507 agreement with the results of previous studies.^{21,47} While hydrolytic activity of PefL on
508 PBAT50 was previously reported,²⁴ this activity was observed at $T_{\text{exp}} = 50^{\circ}\text{C}$. The lower
509 $T_{\text{exp}} = 30^{\circ}\text{C}$ used herein likely explains why we did not detect activity of PefL on
510 PBAT50 in the QCM-D experiment.

511 Based on the crystallographic structures available for seven of the eight tested
512 carboxylesterases, we employed published algorithms to compute the surface area of
513 the active-site serine in each of the carboxylesterases that was accessible to probes of
514 varying radii. These computations showed that the active sites of FsC and TcC, the two
515 enzymes that hydrolyzed PBAT50, were more accessible than the active sites of RoL,
516 PefL, and CbE, three of the enzymes that did not hydrolyze PBAT50 (**Figure S17**). The
517 computations for these five enzymes therefore support that active-site accessibility is
518 an important parameter that governs the hydrolytic activity of carboxylesterases on
519 polyesters, particularly on aromatic-aliphatic co-polyesters with high ratios of aromatic
520 to aliphatic diacid components.^{18,31,35} Future work may extend this concept to additional
521 enzymes and polyesters. For example, we expect that the PETase recently identified by
522 Yoshida et al. has a highly accessible active site, given its high hydrolytic activity on
523 poly(ethylene terephthalate).²⁶

Implications. This work demonstrated that QCM-D measurements allow following enzymatic polyester hydrolysis at the nanometer scale with high sensitivity and in real time. Through systematic variations in the chemical composition of the tested polyesters and by comparing different carboxylesterases, we showed that the physicochemical and structural properties of both the polyester and the carboxylesterase determine the rates and extents of enzymatic polyester hydrolysis. The results of this work call for experimental and modeling studies that specifically investigate the critical interplay between polyester chain flexibility and enzyme active-site accessibility.

Our QCM-D measurements demonstrated that a nanoscale non-uniformity in the physicochemical properties affected the enzymatic hydrolyzability of polyester films. This finding motivates future studies that investigate the processes that give rise non-uniformity, characterize the physicochemical properties of different domains in non-uniform polyesters, and link these properties to enzymatic hydrolyzability. A more thorough characterization of polyester non-uniformity at the nanoscale is important not only to advance our mechanistic understanding of enzymatic polyester hydrolysis but also to provide new avenues to designing polyesters with optimized structural stability and biodegradability.

Associated content

Supporting Information. Additional information and data on used chemicals, QCM-D and pH-stat titration experiments. This material is available free of charge via the Internet at <http://pubs.acs.org>.

Author information.

Corresponding author: * Email: michael.sander@env.ethz.ch

Notes

The authors declare no competing financial interest.

Acknowledgements.

We thank Prof. David Norris and Jan Winkler for access to the spin coater and Felix Schmidt for the help with hydrolysis experiments. MZ, MS, KMN and HPK thank the Joint Research Network on Advanced Materials and Systems (JONAS) program of BASF SE and ETH Zurich for scientific and financial support. VP, DR, and GG acknowledge support by the Federal Ministry of Science, Research and Economy (BMFWF), the Federal Ministry of Traffic, Innovation and Technology (bmvit), the Styrian Business Promotion Agency SFG, the Standortagentur Tirol, the Government of Lower Austria, and Business Agency Vienna through the COMET-Funding Program managed by the Austrian Research Promotion Agency FFG.

References

- (1) Shah, A. A.; Kato, S.; Shintani, N.; Kamini, N. R.; Nakajima-Kambe, T. Microbial degradation of aliphatic and aliphatic-aromatic co-polyesters. *Appl. Microbiol. Biotechnol.* **2014**, *98* (8), 3437–3447.
- (2) Russell, J. R.; Huang, J.; Anand, P.; Kucera, K.; Sandoval, A. G.; Dantzler, K. W.; Hickman, D.; Jee, J.; Kimovec, F. M.; Koppstein, D.; Marks, D. H.; Mittermiller, P. A.; Nunez, S. J.; Santiago, M.; Townes, M. A.; Vishnevetsky, M.; Williams, N. E.; Vargas, M. P. N.; Boulanger, L. A.; Bascom-Slack, C.; Strobel, S. A. Biodegradation of Polyester Polyurethane by Endophytic Fungi. *Appl. Environ. Microb.* **2011**, *77* (17), 6076–6084.
- (3) Thompson, R. C.; Olsen, Y.; Mitchell, R. P.; Davis, A.; Rowland, S. J.; John, A. W. G.; McGonigle, D.; Russell, A. E. Lost at sea: where is all the plastic? *Science* **2004**, *304* (5672), 838.
- (4) Rillig, M. C. Microplastic in Terrestrial Ecosystems and the Soil? *Environ. Sci. Technol.* **2012**, *46* (12), 6453–6454.
- (5) Puoci, F.; Iemma, F.; Spizzirri, U. G.; Cirillo, G.; Curcio, M.; Picci, N. Polymer in agriculture: a review. *American Journal of Agricultural and Biological Sciences* **2008**, *3* (1), 299–314.
- (6) Nizzetto, L.; Futter, M.; Langaas, S. Are Agricultural Soils Dumps for Microplastics of Urban Origin? *Environ. Sci. Technol.* **2016**, *50* (20), 10777–10779.
- (7) Liu, E. K.; He, W. Q.; Yan, C. R. ‘White revolution’ to ‘white pollution’—agricultural plastic film mulch in China. *Environ. Res. Lett.* **2014**, *9* (9), 1–4.
- (8) Kyrikou, I.; Briassoulis, D. Biodegradation of Agricultural Plastic Films: A Critical Review. *J. Polym. Environ.* **2007**, *15* (2), 125–150.
- (9) Briassoulis, D.; Dejean, C.; Picuno, P. Critical Review of Norms and Standards for Biodegradable Agricultural Plastics Part II: Composting. *J.*

- 588 *Polym. Environ.* **2010**, 18 (3), 364–383.
- 589 (10) Gross, R. A. Biodegradable Polymers for the Environment. *Science* **2002**, 297
- 590 (5582), 803–807.
- 591 (11) Sintim, H. Y.; Flury, M. Is Biodegradable Plastic Mulch the Solution to
- 592 Agriculture's Plastic Problem? *Environ. Sci. Technol.* **2017**, 51 (3), 1068–
- 593 1069.
- 594 (12) Künkel, A.; Becker, J.; Börger, L.; Hamprecht, J.; Koltzenburg, S.; Loos, R.;
- 595 Schick, M. B.; Schlegel, K.; Sinkel, C.; Skupin, G.; Monotori, Y. *Ullmann's*
- 596 *Encyclopedia of Industrial Chemistry*; Wiley-VCH Verlag GmbH & Co.
- 597 KGaA: Weinheim, 2016; pp 1–29.
- 598 (13) Müller, R.-J.; Kleeberg, I.; Deckwer, W.-D. Biodegradation of polyesters
- 599 containing aromatic constituents. *J. Biotechnol.* **2001**, 86 (2), 87–95.
- 600 (14) Witt, U.; Einig, T.; Yamamoto, M.; Kleeberg, I.; Deckwer, W. D.; Müller, R.
- 601 J. Biodegradation of aliphatic–aromatic copolyesters: evaluation of the final
- 602 biodegradability and ecotoxicological impact of degradation intermediates.
- 603 *Chemosphere* **2001**, 44 (2), 289–299.
- 604 (15) Witt, U.; Müller, R. J.; Deckwer, W. D. Biodegradation of Polyester
- 605 Copolymers Containing Aromatic Compounds. *Journal of Macromolecular*
- 606 *Science, Part A* **1995**, 32 (4), 851–856.
- 607 (16) Breulmann, M.; Künkel, A.; Philipp, S.; Reimer, V.; Siegenthaler, K. O.;
- 608 Skupin, G.; Yamamoto, M. *Ullmann's Encyclopedia of Industrial Chemistry*;
- 609 Wiley-VCH Verlag GmbH & Co. KGaA: Weinheim, 2009; pp 265–294.
- 610 (17) Bornscheuer, U. T. Feeding on plastic. *Science* **2016**, 351 (6278), 1154–1155.
- 611 (18) Mueller, R.-J. Biological degradation of synthetic polyesters—Enzymes as
- 612 potential catalysts for polyester recycling. *Process Biochem.* **2006**, 41 (10),
- 613 2124–2128.
- 614 (19) Yamamoto-Tamura, K.; Hiradate, S.; Watanabe, T.; Koitabashi, M.;
- 615 Sameshima-Yamashita, Y.; Yarimizu, T.; Kitamoto, H. Contribution of soil
- 616 esterase to biodegradation of aliphatic polyester agricultural mulch film in
- 617 cultivated soils. *AMB Express* **2015**, 5 (1), 10.
- 618 (20) Tokiwa, Y.; Suzuki, T. Hydrolysis of polyesters by lipases. *Nature* **1977**, 270
- 619 (5632), 76–78.
- 620 (21) Perz, V.; Hromic, A.; Baumschlager, A.; Steinkellner, G.; Pavkov-Keller, T.;
- 621 Gruber, K.; Bleymaier, K.; Zitzenbacher, S.; Zankel, A.; Mayrhofer, C.;
- 622 Sinkel, C.; Küper, U.; Schlegel, K.; Ribitsch, D.; Guebitz, G. M. An esterase
- 623 from anaerobic *Clostridium hathewayi* can hydrolyze aliphatic aromatic
- 624 polyesters. *Environ. Sci. Technol.* **2016**, 50 (6), 2899–2907
- 625 (22) Perz, V.; Baumschlager, A.; Bleymaier, K.; Zitzenbacher, S.; Hromic, A.;
- 626 Steinkellner, G.; Pairitsch, A.; Łyskowski, A.; Gruber, K.; Sinkel, C.; Küper,
- 627 U.; Ribitsch, D.; Guebitz, G. M. Hydrolysis of Synthetic Polyesters by
- 628 *Clostridium botulinum* Esterases. *Biotechnol. Bioeng.* **2015**, 113 (5), 1024–
- 629 1034.
- 630 (23) Perz, V.; Bleymaier, K.; Sinkel, C.; Kueper, U.; Bonnekessel, M.; Ribitsch,
- 631 D.; Guebitz, G. M. Substrate specificities of cutinases on aliphatic-aromatic
- 632 polyesters and on their model substrates. *N. Biotechnol.* **2016**, 33 (2), 295–
- 633 304.
- 634 (24) Biundo, A.; Hromic, A.; Pavkov-Keller, T.; Gruber, K.; Quartinello, F.;
- 635 Haernvall, K.; Perz, V.; Arrell, M. S.; Zinn, M.; Ribitsch, D.; Guebitz, G. M.
- 636 Characterization of a poly(butylene adipate-co-terephthalate)-hydrolyzing
- 637 lipase from *Pelosinus fermentans*. *Appl. Microbiol. Biotechnol.* **2015**, 100 (4),

- 1753–1764.
- (25) Kleeberg, I.; Welzel, K.; VandenHeuvel, J.; Müller, R. J.; Deckwer, W. D. Characterization of a New Extracellular Hydrolase from *Thermobifida fusca* Degrading Aliphatic–Aromatic Copolyesters. *Biomacromolecules* **2005**, *6* (1), 262–270.
- (26) Yoshida, S.; Hiraga, K.; Takehana, T.; Taniguchi, I.; Yamaji, H.; Maeda, Y.; Toyohara, K.; Miyamoto, K.; Kimura, Y.; Oda, K. A bacterium that degrades and assimilates poly(ethylene terephthalate). *Science* **2016**, *351* (6278), 1196–1199.
- (27) Marten, E.; Müller, R.-J.; Deckwer, W.-D. Studies on the enzymatic hydrolysis of polyesters I. Low molecular mass model esters and aliphatic polyesters. *Polym. Degrad. Stab.* **2003**, *80* (3), 485–501.
- (28) Rizzarelli, P.; Impallomeni, G.; Montaudo, G. Evidence for Selective Hydrolysis of Aliphatic Copolyesters Induced by Lipase Catalysis. *Biomacromolecules* **2004**, *5* (2), 433–444.
- (29) Herrero Acero, E.; Ribitsch, D.; Steinkellner, G.; Gruber, K.; Greimel, K.; Eiteljoerg, I.; Trotscha, E.; Wei, R.; Zimmermann, W.; Zinn, M.; Cavaco-Paulo, A.; Freddi, G.; Schwab, H.; Guebitz, G. M. Enzymatic Surface Hydrolysis of PET: Effect of Structural Diversity on Kinetic Properties of Cutinases from *Thermobifida*. *Macromolecules* **2011**, *44* (12), 4632–4640.
- (30) Ribitsch, D.; Yebra, A. O.; Zitzenbacher, S.; Wu, J.; Nowitsch, S.; Steinkellner, G.; Greimel, K.; Doliska, A.; Oberdorfer, G.; Gruber, C. C.; Schwab, H.; Stana-Kleinshek, K.; Herrero Acero, E.; Guebitz, G.M. Fusion of Binding Domains to *Thermobifida cellulosilytica* Cutinase to Tune Sorption Characteristics and Enhancing PET Hydrolysis. *Biomacromolecules* **2013**, *14* (6), 1769–1776.
- (31) Zumstein, M. T.; Kohler, H.-P. E.; McNeill, K.; Sander, M. High-Throughput Analysis of Enzymatic Hydrolysis of Biodegradable Polyesters by Monitoring Cohydrolysis of a Polyester-Embedded Fluorogenic Probe. *Environ Sci Technol* **2017**, *51* (8), 4358–4367.
- (32) Zumstein, M. T.; Kohler, H.-P. E.; McNeill, K.; Sander, M. Enzymatic Hydrolysis of Polyester Thin Films: Real-Time Analysis of Film Mass Changes and Dissipation Dynamics. *Environ. Sci. Technol.* **2016**, *50* (1), 197–206.
- (33) Tokiwa, Y.; Suzuki, T.; Takeda, K. Two Types of Lipases in Hydrolysis of Polyester. *Agric. Biol. Chem.* **1988**, *52* (8), 1937–1943.
- (34) Marten, E.; Müller, R.-J.; Deckwer, W.-D. Studies on the enzymatic hydrolysis of polyesters. II. Aliphatic–aromatic copolyesters. *Polym. Degrad. Stab.* **2005**, *88* (3), 371–381.
- (35) Araujo, R.; Silva, C.; O'Neill, A.; Micaelo, N.; Guebitz, G.; Soares, C. M.; Casal, M.; Cavaco-Paulo, A. Tailoring cutinase activity towards polyethylene terephthalate and polyamide 6,6 fibers. *J. Biotechnol.* **2007**, *128* (4), 849–857.
- (36) Silva, C.; Da, S.; Silva, N.; Matamá, T.; Araujo, R.; Martins, M.; Chen, S.; Chen, J.; Wu, J.; Casal, M.; Cavaco-Paulo, A. Engineered *Thermobifida fusca* cutinase with increased activity on polyester substrates. *Biotechnol. J.* **2011**, *6* (10), 1230–1239.
- (37) Lindström, A.; Albertsson, A.-C.; Hakkarainen, M. Quantitative determination of degradation products an effective means to study early stages of degradation in linear and branched poly(butylene adipate) and

- poly(butylene succinate). *Polym. Degrad. Stab.* **2004**, 83 (3), 487–493.
- (38) Gan, Z.; Kuwabara, K.; Yamamoto, M.; Abe, H.; Doi, Y. Solid-state structures and thermal properties of aliphatic–aromatic poly(butylene adipate-co-butylene terephthalate) copolyesters. *Polym. Degrad. Stab.* **2004**, 83 (2), 289–300.
- (39) Ribitsch, D.; Herrero Acero, E.; Greimel, K.; Dellacher, A.; Zitzenbacher, S.; Marold, A.; Rodriguez, R. D.; Steinkellner, G.; Gruber, K.; Schwab, H.; Guebitz, G.M. A New Esterase from *Thermobifida halotolerans* Hydrolyses Polyethylene Terephthalate (PET) and Polylactic Acid (PLA). *Polymers* **2012**, 4 (4), 617–629.
- (40) Armanious, A.; Aeppli, M.; Sander, M. Dissolved Organic Matter Adsorption to Model Surfaces: Adlayer Formation, Properties, and Dynamics at the Nanoscale. *Environ. Sci. Technol.* **2014**, 48 (16), 9420–9429.
- (41) Vörös, J. The Density and Refractive Index of Adsorbing Protein Layers. *Biophys. J.* **2004**, 87 (1), 553–561.
- (42) Sander, M.; Madliger, M.; Schwarzenbach, R. P. Adsorption of Transgenic Insecticidal Cry1Ab Protein to SiO₂. 1. Forces Driving Adsorption. *Environ. Sci. Technol.* **2010**, 44 (23), 8870–8876.
- (43) Muroi, F.; Tachibana, Y.; Soulethone, P.; Yamamoto, K.; Mizuno, T.; Sakurai, T.; Kobayashi, Y.; Kasuya, K.-I. Characterization of a poly(butylene adipate-co-terephthalate) hydrolase from the aerobic mesophilic bacterium *Bacillus pumilus*. *Polym. Degrad. Stab.* **2017**, 137, 11–22.
- (44) Chen, S.; Su, L.; Chen, J.; Wu, J. Cutinase: characteristics, preparation, and application. *Biotechnol. Adv.* **2013**, 31 (8), 1754–1767.
- (45) Dutta, K.; Sen, S.; Veeranki, V. D. Production, characterization and applications of microbial cutinases. *Process Biochem.* **2009**, 44 (2), 127–134.
- (46) Jaeger, K.-E.; Ransac, S.; Dijkstra, B. W.; Colson, C.; van Heuvel, M.; Misset, O. Bacterial lipases. *FEMS Microbiol. Rev.* **1994**, 15 (1), 29–63.
- (47) Perz, V.; Bleymaier, K.; Sinkel, C.; Kueper, U.; Bonnekessel, M.; Ribitsch, D.; Guebitz, G. M. Substrate specificities of cutinases on aliphatic–aromatic polyesters and on their model substrates. *N. Biotechnol.* **2015**, 33 (2), 1–10.